Journal of Arrhythmia 31 (2015) 352–358

Contents lists available at ScienceDirect

Journal of Arrhythmia

journal homepage: www.elsevier.com/locate/joa

Original Article

Effects of a high-fat diet on the electrical properties of porcine atria

Yasuo Okumura, MD[a,*], Ichiro Watanabe, MD[a], Koichi Nagashima, MD[a], Kazumasa Sonoda, MD[a], Naoko Sasaki, MD[a], Rikitake Kogawa, MD[a], Keiko Takahashi, MD[a], Kazuki Iso, MD[a], Kimie Ohkubo, MD[a], Toshiko Nakai, MD[a], Rie Takahashi [b], Yoshiki Taniguchi [c], Masako Mitsumata, MD[d], Mizuki Nikaido, BE[e], Atsushi Hirayama, MD[a]

[a] Division of Cardiology, Department of Medicine, Nihon University School of Medicine, Ohyaguchi-kamicho, Itabashi-ku, Tokyo 173-8610, Japan
[b] Department of Advanced Cardiovascular Imaging, Nihon University School of Medicine, Tokyo, Japan
[c] Institute of Medical Science, Medical Research Support Center, Section of Laboratory for Animal Experiments, Nihon University School of Medicine, Tokyo, Japan
[d] Department of Pathology, Nihon University School of Medicine, Tokyo, Japan
[e] Nihon Kohden Corporation Tokyo, Japan

ARTICLE INFO

Article history:
Received 13 February 2015
Received in revised form
6 April 2015
Accepted 11 May 2015
Available online 17 June 2015

Keywords:
Atrial fibrillation
High-fat diet
Electrical properties

ABSTRACT

Background: Because obesity is an important risk factor for atrial fibrillation (AF), we conducted an animal study to examine the effect of a high-fat diet (HFD) on atrial properties and AF inducibility.
Methods: Ten 8-week-old pigs (weight, 18–23 kg) were divided into two groups. For 18 weeks, five pigs were fed a HFD (HFD group) and five were fed a normal diet (control group). Maps of atrial activation and voltages during sinus rhythm were created for all pigs using the EnSite NavX system. Effective refractory period (ERP) and AF inducibility were also determined. When AF was induced, complex fractionated atrial electrogram (CFAE) mapping was performed. At 18 weeks, hearts were removed for comparing the results of histological analysis between the two groups. Body weight, lipid levels, hemodynamics, cardiac structures, and electrophysiological properties were also compared.
Results: Total cholesterol levels were significantly higher (347 [191–434] *vs.* 81 [67–88] mg/dL, $P=0.0088$), and left atrium pressure was higher (34.5 [25.6–39.5] *vs.* 24.5 [21.3–27.8] mmHg, $P=0.0833$) in the HFD group than in the control group, although body weight only increased marginally (89 [78–101] *vs.* 70 [66–91] kg, $P=0.3472$). ERPs of the pulmonary vein (PV) were shorter ($P<0.05$) and AF lasted longer in the HFD group than in the control group (80 [45–1350] *vs.* 22 [3–30] s, $P=0.0212$). Neither CFAE site distribution nor histopathological characteristics differed between the two groups.
Conclusions: The shorter ERPs for the PV observed in response to the HFD increased vulnerability to AF, and these electrophysiological characteristics may underlie obesity-related AF.

1. Introduction

Metabolic syndrome comprises a cluster of conditions, including obesity, insulin resistance, hypertension, and abnormal cholesterol levels, which together increase cardiovascular risk. Metabolic syndrome and obesity have been reported to promote systemic inflammation and oxidative stress [1,2], and patients with metabolic syndrome have increased epicardial adipose tissue volumes [3]. The systemic and local conditions related to obesity and metabolic syndrome have been linked to the pathogenesis of atrial fibrillation (AF) [4–6]. In fact, numerous epidemiological studies have shown that obesity, one of the components of metabolic syndrome, is associated with both the new onset and progression of AF [7–9]. However, the mechanism explaining the link between obesity or metabolic syndrome and AF progression is unclear. To elucidate this mechanism, we investigated electrophysiological properties and vulnerability to AF in pigs fed on a high-fat diet (HFD).

2. Material and methods

2.1. Animal preparation

The experimental protocol was approved by the Institutional Animal Care and Use Committee of the Nihon University School of Medicine. Ten 8-week-old domestic pigs (weight, 18–23 kg) were divided into two groups. Five pigs were fed a normal diet for 18 weeks (control group) and five were fed a HFD for 18 weeks (HFD group). The pigs were housed in individual cages (1.25 m^3) under

* Corresponding author. Tel.: +81 3 3972 8111; fax: +81 3 3972 1098.
E-mail address: yasuwo128@yahoo.co.jp (Y. Okumura).

http://dx.doi.org/10.1016/j.joa.2015.05.004
1880-4276/

controlled conditions (23 ± 0. 5 °C, 55 ± 5% humidity, and 12 h of light from 06:00 to 18:00). The animals in the control group were fed a commercial diet (PiguMiral CEX, JA Higashinihon Kumiai Shiryou, Co., Ltd., Gunma, Japan), which consisted of 71% cereal, 12% vegetable-origin oilseed, 6% chaff and bran, and 11% vitamins and minerals. The animals in the HFD group were fed a HFD, which consisted of 25% lard, 2.5% cholesterol, 20% granulated sugar, and 52.5% commercial feed (described above). In both groups, the daily food volume intake was 1 kg from week 8 to week 10, and 2 kg from week 11 to week 18. End-study (18-week) body weight, systolic and diastolic blood pressure, heart rate, and mean left atrial pressure were obtained from all animals. Blood samples were taken, and lipids were assessed by a commercial laboratory (SRL, Inc., Tokyo, Japan). In preparation for intracardiac echocardiography (ICE) and electrophysiology study (EPS) assessments, the animals were anesthetized with an intramuscular injection of 0.1 mg/kg midazolam, which was followed by inhalation of 5% isoflurane and then 1–3% isoflurane for maintenance. A tracheal cannula was inserted, and intermittent positive-pressure ventilation (room air, tidal volume, 10 mL/kg; rate, 20 breaths/min) was provided using a respirator. After deep anesthesia was established, vascular access was obtained percutaneously via the right external jugular vein and the right and left femoral veins and artery. Surface electrocardiograms (ECGs) and blood pressure were monitored continuously throughout the procedures. A 7-Fr catheter was positioned in the distal coronary sinus (CS) for anatomical guidance, and to provide a reference for the timing of data acquisition. A 10-Fr, 64-element, 5.5–10.0-MHz, phased-array ICE catheter, which works with the Vivid 7 system (GE Healthcare Technologies, Wauwatosa, WI, USA), was advanced to the level of the tricuspid annulus to measure the left atrium (LA) and left ventricle (LV), and to guide transseptal catheterization.

2.2. ICE

ICE was performed before EPS. All recordings were taken in sinus rhythm (SR). The short and long axes of the LA were measured from a 2-dimensional (2D) ICE image (long-axis view); the LV ejection fraction, LV end-systolic and diastolic dimensions, and interventricular septum and posterior wall dimensions were also measured from the 2D ICE image (short-axis view).

2.3. EPS

Transseptal catheterization was accomplished under fluoroscopic and ICE guidance. After transseptal puncture, left atrial pressure was measured, and an Agilis deflectable long sheath (St. Jude Medical, Inc., St. Paul, MN, USA) was inserted into the LA. The 3-dimensional (3D) geometry of the right atrium (RA), LA, and four pulmonary veins (PVs) was reconstructed using the EnSite NavX system, version 8.0 (St. Jude Medical, Inc.). A 20-pole circular mapping catheter with 1.5-mm interelectrode spacing (Livewire Spiral HP Catheter, St. Jude Medical, Inc.) and 8-pole mapping catheter with 4-mm interelectrode spacing (Snake, Japan Lifeline, Inc., Tokyo, Japan) were used for the mapping and creation of the 3D geometry. A 3D activation map was created during the acquisition of bipolar signals (filter setting, 30–500 Hz) from the 20-pole circular mapping catheter. Electrograms recorded during SR were stored and analyzed offline with the NavX mapping system. Bipolar voltage amplitudes derived from two to three mapping points were averaged for each of the following 13 LA/PV segments: superior vena cava (SVC); SVC–RA junction; right atrial appendage (RAA); lateral and septal RA; septal and posterior LA and LA roof; mitral isthmus; left atrial appendage (LAA); and the orifices of the right and left superior PVs and common inferior PVs. Potentials with amplitudes >0.5 mV were deemed normal-voltage potentials and coded in purple, and potentials with amplitudes <0.2 mV were deemed low-voltage potentials and coded in red or grey [10]. The effective refractory period (ERP) (longest premature coupling interval [S1–S2] that failed to capture) was measured from both atria ($2\times$ threshold current, 2-ms pulses) at basic cycle lengths of 400 ms with eight basic stimuli (S1), followed by premature (S2) stimuli in 10-ms decrements. ERPs were obtained at six different locations (the RAA, SVC–RA junction, LAA, and orifices of the right and left superior PVs and common inferior PVs). At each site, the ERP was measured three times and averaged. AF was induced by 5-s burst pacing (10 Hz; $4\times$ threshold current), and the duration of sustained AF was measured. If AF lasting >30 s was induced repeatedly, a complex fractionated atrial electrogram (CFAE) map was created during AF. For CFAE analysis, the NavX mapping parameters were set to the CFAE-mean, an algorithm was used to determine the average index of the fractionation at each site, and a color map of the fractionation intervals (FIs) (CFAE map) was constructed [11–13]. The FI was taken as the average time between consecutive deflections over a 5-s recording period. The settings included a refractory period of 30 ms (adjusted for animals from the clinical setting of 40 ms), peak-to-peak sensitivity between 0.05 mV and 0.1 mV, and an electrogram duration of <10 ms. Continuous CFAEs were defined as those with a mean FI of <50 ms and variable CFAEs as those with an FI of 50–120 ms.

2.4. Histopathological analysis

After ICE and EPS, all animals were euthanized and their hearts were removed, fixed in 10% formalin, and subjected to histological analysis. Paraffin-embedded specimens were serially sectioned as 4-μm slices for staining with hematoxylin–eosin and Masson's trichrome. The sections were examined for fibrotic or inflammatory changes or myocyte hypertrophy present at the SVC–RA junction, RAA, lateral RA, posterior LA, LA roof, LAA, and the orifices of the right and left superior PVs and common inferior PVs. An expert pathologist (M.M.) twice interpreted at least one or two slides.

2.5. Statistical analysis

Continuous variables were expressed as median values with interquartile ranges. Between-group differences in continuous variables were analyzed using the Mann–Whitney *U* test. A *P*-value of <0.05 was considered statistically significant. All statistical analyses were performed with JMP 11. 2.0 software (SAS Institute Inc., Cary, NC).

3. Results

3.1. End-study body weight and hemodynamic variables, ICE measurements, and lipid levels

Animals' end-study body weights, hemodynamic variables, and ICE measurements are shown for each group in Table 1. The end-study body weight was 89 [78–101] kg in the HFD group and only marginally greater than that in the control group (70 [66–91] kg, $P=0.3472$). The mean LA pressure tended to be higher in the HFD group than in the control group (34.5 [25.6–39.5] *vs.* 24.5 [21.3–27.8] mmHg, $P=0.0833$). There were no differences in other hemodynamic variables or the ICE measurements between the two groups. As expected, the following lipid levels were significantly higher in the HFD group than in the control group: total cholesterol (347 [191–434] mg/dL *vs.* 81 [67–88] mg/dl, $P=0.0088$), low-density lipoprotein cholesterol (LDL) (276 [115–340] mg/dL *vs.* 43 [34–48] mg/dL, $P=0.0163$) and high-

Table 1
End-study[a] body weight, hemodynamic variables, and ICE measurements in the study groups.

	Control ($n=5$)	HFD ($n=5$)	P-value
Body weight (kg)	70 [66–91]	89 [78–101]	0.3472
Systolic BP (mmHg)	120 [94–140]	130 [114–150]	0.3472
Diastolic BP (mmHg)	70 [58–82]	81 [62–95]	0.3472
Heart rate (beats/min)	114 [98–141]	128 [115–140]	0.6015
Mean LA pressure (mmHg)	24.5 [21.3–27.8]	34.5 [25.6–39.5]	0.0833
LAD short (mm)	31 [29–34]	30 [26–33]	0.6714
LAD long (mm)	40 [35–41]	37 [34–47]	0.5959
IVSd (mm)	9.0 [7.0–10.0]	10.0 [7.5–13.5]	0.2888
PWd (mm)	10.0 [8.5–11.5]	13.0 [9.5–13.5]	0.1706
LVEF (%)	66.5 [65.0–66.0]	70.0 [65.3–82.3]	0.2248

Values are shown as median [Q1–Q3].
Control; normal diet; HFD, high-fat diet; ICE, intracardiac echocardiography; LAD, left atrial dimension; LVEF, left ventricular ejection fraction; IVSd, interventricular septum dimension; PWd, posterior wall dimension.

[a] End of the 18-week dietary period.

density lipoprotein cholesterol (HDL) (58 [41–74] mg/dL *vs.* 30 [29–41] mg/dL, $P=0.0278$). However, no difference was noted in triglyceride levels (17 [14–27] mg/dL *vs.* 22 [16–30] mg/dL, $P=0.4620$).

3.2. EPS evaluation

A total of 310 ± 113 mapping points were acquired per case for the creation of the 3D geometric voltage maps during SR. Representative 3D voltage maps from the control group and HFD group are shown in Fig. 1A. Total atrial conduction time, which was defined as the time from the onset of the P wave in lead II of the surface ECG to the atrial signal at the distal electrodes of the CS catheter, did not differ between the two groups. Regionally, in both groups, bipolar voltage amplitudes at the SVC, SVC–RA junction, and orifices of the three PVs were lower than those at other sites, but there was no between-group difference in bipolar voltage amplitudes at any site (Table 2). ERPs at the thoracic veins were significantly shorter in the HFD group than in the control group, whereas ERPs at the RAA and LAA were marginally shorter in the HFD group than in the control group (Table 2). Burst pacing was used to induce AF in all animals, but AF lasted significantly longer in the HFD group than in the control group (80 [44.5–1350] s *vs.* 22 [2.8–29.5] s, $P=0.0212$). A CFAE map (213 ± 47 points) was created for all animals in the HDF group but for only two animals in the control group because AF was not repeatedly sustained by burst pacing in these animals. Representative CFAE maps from the two groups are shown in Fig. 1B. Regionally, CFAE sites were similarly distributed in the two groups and were located at the RA appendage, SVC–RA junction, left superior PV orifice, posterior LA, and LA appendage more frequently than at the thoracic veins.

3.3. Histopathological findings

Upon gross examination, no specific histopathological changes were seen in any animal. Even at the SVC–RA junction and LA near the PV orifices (left and right panels in Fig. 2), representing CFAE sites in the both groups, there were no histological abnormalities such as fatty or inflammatory changes or hypertrophied myocytes. Despite the meticulous histopathological assessment of all sections, no myocardial fibrosis, *i.e.*, areas of myocyte loss replaced by fibrotic tissue, was found in either group (Fig. 3). In both groups, ganglions or nerve fiber bundles were seen at sites adjacent to the SVC–RA junction or PV orifices (Fig. 2), and neither the number nor distribution differed between the two groups.

4. Discussion

4.1. Main findings

An important finding of the study was that ERPs of the thoracic veins, including the PV orifices and SVC, were significantly shorter in the HFD group than in the control group. Furthermore, inducibility and duration of AF were higher in the HFD group than in the control group. Nonetheless, no specific differences were found in the bipolar signals during SR and AF or in the characteristics of studied tissues between the two groups.

4.2. Effect of the HFD on atrial electrical properties

The electrophysiological properties related to AF maintenance include shortening and loss of rate adaptation during the atrial refractory period and prolonged atrial conduction time [14–16]. The pronounced inducibility and duration of sustained AF documented in our HFD group may have been due to the shortening of ERPs at the PV orifices. This electrical property, referred to as “electrical remodeling”, has been reported to represent the early stage of AF progression [14–16]. Furthermore, electrical remodeling was more significantly pronounced in the thoracic veins such as the PVs and SVC than in the atria, and this observation is consistent with the reported characteristics of atrial remodeling in humans with AF [17–19]. The mechanism underlying shortening of the ERPs in the HFD group is unclear. The HFD group had significantly higher total cholesterol, LDL, and HDL cholesterol levels than the control group. Elevated LDL cholesterol is a causal risk factor for cardiovascular disease, but in recent epidemiological studies, even a low HDL cholesterol or low LDL cholesterol level was associated with an increased risk of AF [20–22]. An inverse relationship between high cholesterol and the incidence of AF was evident even after adjustment for residual confounding factors such as diabetes, hypertension, and statin use [20–22]. Thus, high cholesterol levels may not explain the vulnerability to AF in our HFD group. One potential mechanism explaining shortening of the ERPs in the PV orifices is stretching of the atria and PV myocytes. Animals in the HFD group had slightly greater body weight, blood pressure, and average LA pressure, although the values were not significant compared to control group values. Such underlying conditions yield atrial and PV stretch. It is well known that atrial and PV stretch can play an important role in the development and maintenance of AF [19,23–26]. Acute atrial stretch reduces the atrial refractory period and action potential duration, and reduces atrial conduction velocity, most likely by reducing cellular excitability via the opening of stretch-activated channels [23,24]. In an optical mapping study conducted by Kalifa et al. [25], AF was induced during gradual increases in atrial pressure. At relatively high atrial pressures, the dominant frequency was significantly higher at the LA–PV junction than at the LA free wall, suggesting that re-entry within this area is important for the development of AF. Acute stretch by rapid volume expansion in patients undergoing cardiac surgery was shown to result in conduction slowing across the PV–LA junction, with an increased degree of signal complexity [26]. By promoting re-entry, this substrate may be important in AF initiation and maintenance. Heart rates in the HFD group were higher, though not significantly, than those in the control group. It is possible, that an increase in sympathetic tone affected the electrophysiological properties. In fact, several experimental studies have shown that ERP or action potential duration in atria and PVs is dependent on the balance between parasympathetic and sympathetic nerve tones [27,28]. In a study of electrophysiological properties in obese patients, the ERPs in the proximal and distal PVs were substantially shorter than those in patients with a normal body mass index [19]. These findings also

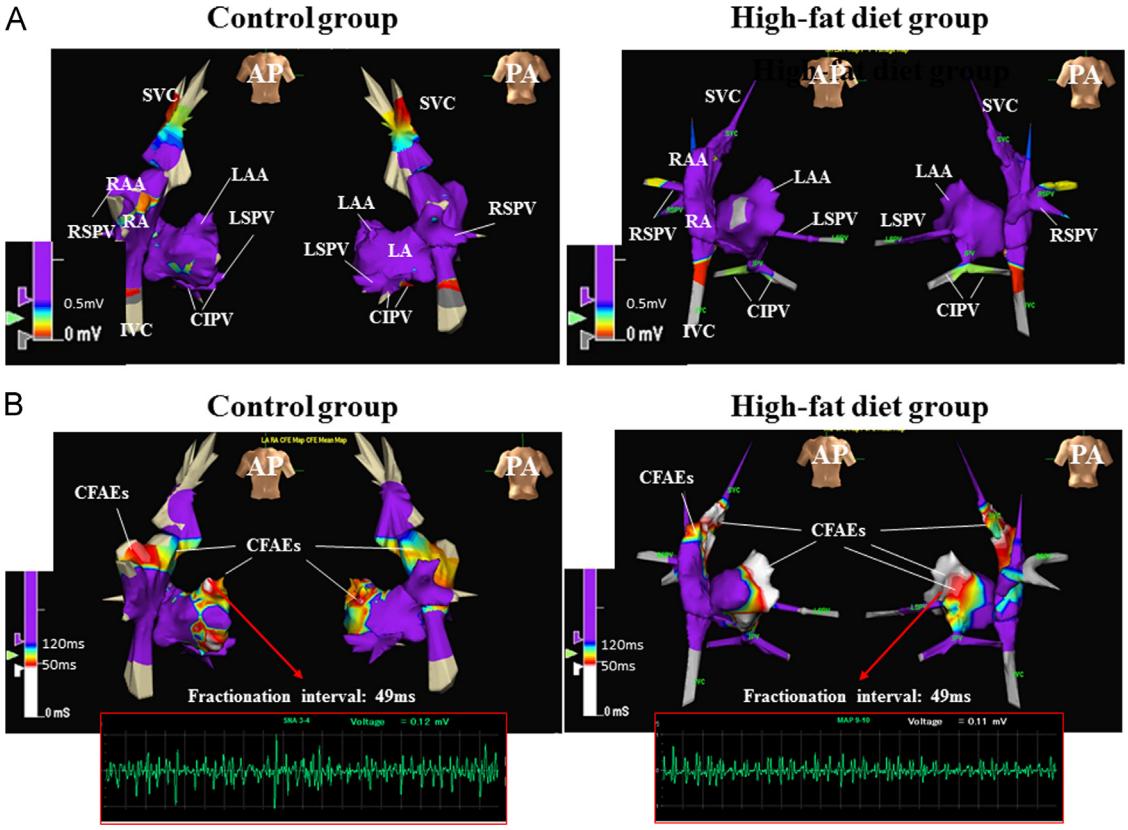

Fig. 1. Representative 3D voltage (A) and complex fractionated atrial electrogram (CFAE) maps (B) from the control group and high-fat diet (HFD) group. (A) No low voltage areas (coded in red or grey) are present at the RA, LA, and PV orifices in either group. Low-voltage areas are absent except at sites deep inside the PVs and IVC in both groups. (B) The distribution of CFAE sites is similar between the two groups, *i.e.*, CFAE sites are located at the RAA, SVC–RA junction, LAA, LA roof, and mitral isthmus in the control animals and at the RAA, SVC–RA junction, LAA, LA roof, posterior LA, and LS–PV orifice in the HFD animals. In both groups, local signals at the LAA show fractionated atrial electrograms, and the fractionation interval at both these sites over a 5-s recording period is 49 ms. AP indicates anterior posterior; PA, posterior anterior; RA, right atrium; RAA, RA appendage; SVC, superior vena cava; IVC, inferior vena cava; LA, left atrium; LAA, LA appendage; PV, pulmonary vein; LS, left superior; CI, common inferior; RS, right superior.

Table 2
Electrophysiological variables in the study groups.

	Control (n=5)	HFD (n=5)	P-value
TACT (ms)	84 [76–100]	77 [67–87]	0.1745
ERPs (ms)			
SVC	180 [170–195]	150 [140–160]	0.0082
RAA	180 [160–180]	140 [125–160]	0.0517
LAA	140 [130–155]	130 [110–135]	0.0827
RSPV orifice	160 [150–175]	130 [110–140]	0.0144
LSPV orifice	160 [145–195]	120 [105–135]	0.0119
CIPV orifice	150 [140–175]	130 [115–140]	0.0232
Voltage amplitude (mV)			
SVC	0.71 [0.45–2.24]	2.31 [0.96–3.26]	0.3472
SVC–RA junction	2.59 [1.50–2.96]	1.96 [1.30–3.63]	0.6752
RAA	5.85 [4.56–6.88]	4.94 [2.95–10.08]	0.9168
RA lateral	3.08 [1.86–5.59]	3.36 [2.69–5.67]	0.7540
RA septum	3.08 [2.07–4.24]	3.45 [1.90–6.76]	0.6015
LA septum	3.52 [1.95–3.79]	4.44 [3.58–5.55]	0.0758
LAA	9.79 [6.25–12.04]	10.62 [7.88–16.99]	0.3472
LA posterior	4.06 [2.79–5.29]	4.31 [1.79–5.89]	0.7540
LA roof	4.17 [2.54–5.29]	4.42 [3.58–4.87]	0.8345
Mitral isthmus	5.93 [5.12–11.5]	10.1 [8.42–10.64]	0.1172
LSPV orifice	1.66 [1.01–2.70]	2.24 [1.55–4.63]	0.2506
RSPV orifice	2.71 [1.90–3.64]	4.23 [2.61–5.11]	0.1745
CIPV orifice	1.54 [1.08–4.12]	3.67 [1.00–5.32]	0.8340

Control, normal diet; HFD, high-fat diet; TACT, total atrial conduction time; ERP, effective refractory period; SVC, superior vena cava; RA, right atrium, RAA RA appendage; LA, left atrium; LAA, LA appendage; PV, pulmonary vein; RS, right superior; LS, left superior; CI, common inferior.

suggested that the shortened ERPs in the PVs are a potential mechanism for sustained or self-perpetuating AF in obese patients. Because obesity is directly linked to inflammation, inflammatory cytokines (*e.g.*, adipocytokines) may have contributed to shortening of the ERPs at the PV orifices in the HFD group. Several adipocytokines, including adiponectin and resistin, have been associated with the presence of AF [29], but there have been few studies regarding the relationship between adipocytokines and the electrophysiological properties underlying vulnerability to AF [30]. In the present study, we did not assess inflammatory markers such as high-sensitivity C-reactive protein or adiponectin. Further studies will be needed to clarify this relationship.

4.3. Atrial structural remodeling in a HFD animal model

Perpetuation of AF causes atrial electrical remodeling in the early stage, subsequently leading to structural remodeling in later stages [16]. Structural remodeling is accompanied by an increase in atrial interstitial fibrosis, hypertrophy, or dilatation. Structural remodeling causes irreversible intra-atrial conduction disturbances, thus promoting AF maintenance. Despite short ERP in the PVs, the HFD diet induced no conduction disturbance or low voltage areas in the atria, or histologically fibrotic or hypertrophied changes in atrial myocytes. Further, AF was more inducible in the HFD group than in the control group, but the duration of sustained AF was relatively short. Contrary to the pigs used in the present study, obese sheep have been shown to have reduced

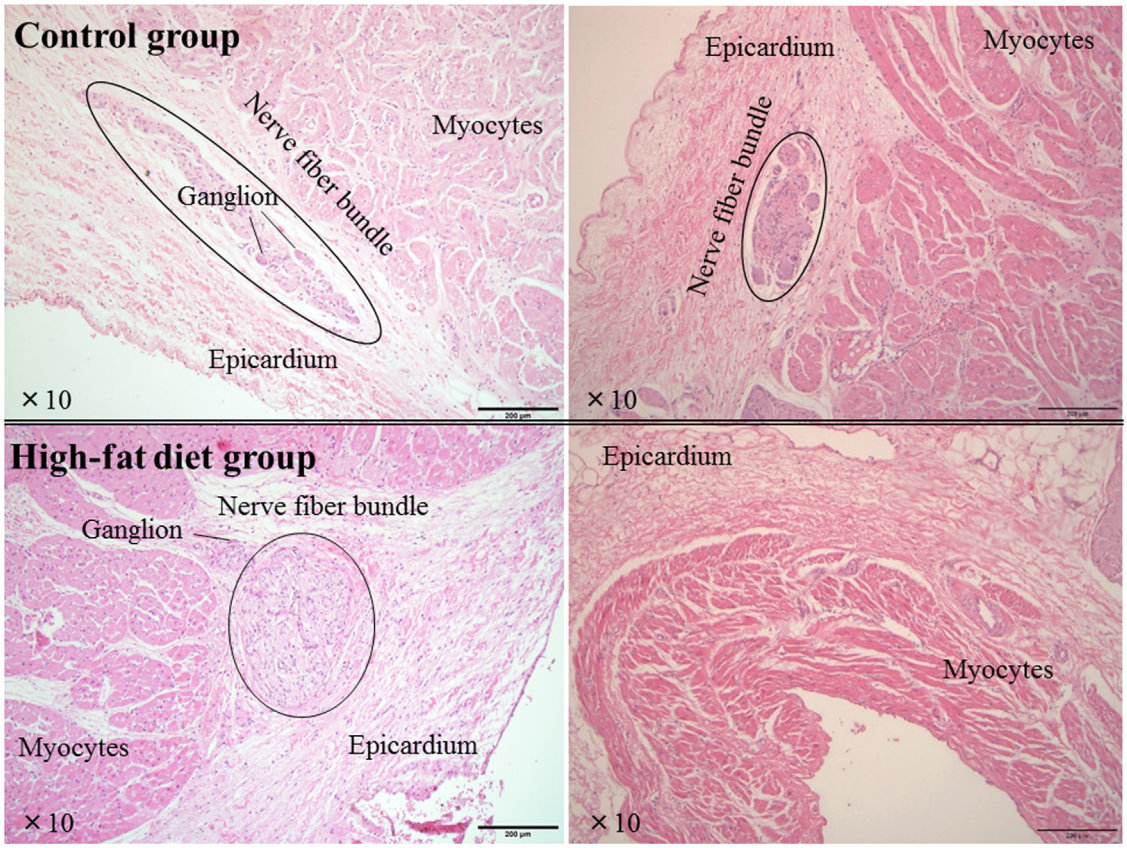

Fig. 2. Representative histopathological slides stained with hematoxylin–eosin of the junction site of the superior vena cava and right atrium (left panels), and left atrium near the left superior pulmonary vein orifice (right panels) in the control group and high-fat diet group. There are no histological abnormalities, *i.e.*, fibrotic, inflammatory, hypertrophic, or fatty changes, in either group. Ganglion or nerve fiber bundles are seen in regions adjacent to the junction site of superior vena cava and right atrium, but no specific differences between the two groups are seen.

conduction velocity and increased conduction heterogeneity for AF-vulnerability [31]. In addition, histological examination showed fibrosis, inflammatory infiltrates, and lipidosis. In the obese sheep model, adult sheep were given a high-calorie diet for 32 weeks, while we used young pigs aged 8 weeks and fed them HFD for 18 weeks. Taken together, these findings suggest that the electrical properties and histological observations in our HFD model may only involve an early stage of electrical remodeling. A longer duration of HFD in adult pigs will be needed to promote structural remodeling.

In the present study, we also investigated the etiology of CFAEs. CFAEs are now considered to result from dyssynchronous activation of separate cell groups at pivot points or wave collision, far-field potentials, or repetitive activations of the AF drivers or local re-entry circuits [11–13,32–34]. In our HFD model, CFAE sites during AF were widely distributed in the RAA, LAA, LA antrum, and LA body rather than in the PVs. In humans with AF, variations in CFAE distribution have been reported, with the distribution dependent on the progression of AF, *i.e.*, CFAEs were predominant in the PVs or PV antra in patients with paroxysmal AF, whereas CFAEs were predominant in the LA body in patients with persistent AF [11,12]. In the present study, CFAE sites did not represent any low voltage areas or histological abnormalities suggestive of a structural abnormality. In AF patients, CFAEs have been reported to be associated with normal bipolar voltage sites in SR [28–30]. These findings imply that even structurally normal tissues can become CFAE sites during AF, and thus, NavX-based CFAE mapping is limited in identifying true AF drivers.

4.4. Limitations

Several study limitations must be considered. First, the study included a small number of animals, which could have influenced our ability to detect statistical differences in several crucial parameters such as body weight and blood pressure. Second, CFAE detection was automatic and based on an algorithm that is part of the NavX software and highly specific. Whether our definition or assessment of CFAE was ideal is debatable, because no studies have assessed CFAE in the porcine atrium. However, we were able to identify fractionated atrial activities at CFAE sites, as shown in Fig. 1. In addition, the algorithm has been validated by catheter ablation results in many studies [11–13,30]. Third, we did not evaluate ion channel function or protein expression by means of the patch-clamp technique or biotechnology. The mechanism of ERP shortening in the HFD group needs further investigation. Finally, we had to work within the technical restrictions of our animal catheterization laboratory, which does not allow animals weighing more than approximately 100 kg. Therefore, we used young pigs and fed them a HFD for a time period that would limit their body weight to approximately 100 kg.

5. Conclusions

Pigs fed an HFD had reduced PV ERPs and increased AF vulnerability, but pathologically normal atrial tissues. These characteristics may in part explain the early-stage electrical remodeling at play in AF maintenance associated with obesity.

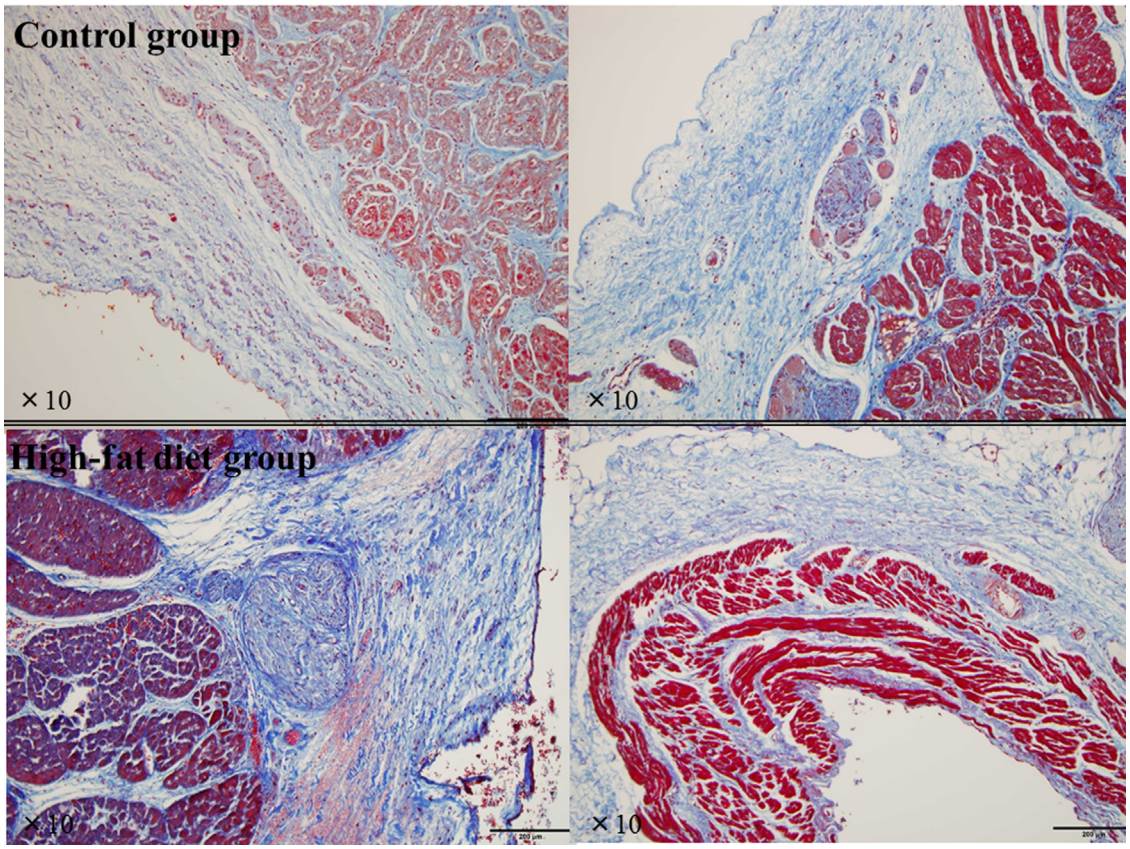

Fig. 3. Representative Masson's trichrome-stained slides of the junction site of the superior vena cava and right atrium (left panels), and left atrium near the left superior pulmonary vein orifice (right panels) in the control group and high-fat diet group. These are the same sections shown in Fig. 2. No myocardial fibrotic tissue replacing areas of myocyte loss is seen in either group.

Conflict of interest

The authors have no conflicts of interest to disclose.

Funding sources

This study was supported in part by a Grant-in-Aid for Scientific Research (KAKENHI) grant.

Acknowledgments

None.

References

[1] Ridker PM, Buring JE, Cook NR, et al. C-reactive protein, the metabolic syndrome, and risk of incident cardiovascular events: an 8-year follow-up of 14,719 initially healthy American women. Circulation 2003;107:391–7.
[2] Ford ES, Mokdad AH, Giles WH, et al. The metabolic syndrome and antioxidant concentrations: findings from the Third National Health and Nutrition Examination Survey. Diabetes 2003;52:2346–52.
[3] Teijeira-Fernandez E, Eiras S, Shamagian LG, et al. Lower epicardial adipose tissue adiponectin in patients with metabolic syndrome. Cytokine 2011;54:185–90.
[4] Nagashima K, Okumura Y, Watanabe I, et al. Association between epicardial adipose tissue volumes on 3-dimensional reconstructed CT images and recurrence of atrial fibrillation after catheter ablation. Circ J 2011;75:2559–65.
[5] Chung MK, Martin DO, Sprecher D, et al. C-reactive protein elevation in patients with atrial arrhythmias: inflammatory mechanisms and persistence of atrial fibrillation. Circulation 2001;104:2886–91.
[6] Mihm MJ, Yu F, Carnes CA, et al. Impaired myofibrillar energetics and oxidative injury during human atrial fibrillation. Circulation 2001;104:174–80.
[7] Benjamin EJ, Levy D, Vaziri SM, et al. Independent risk factors for atrial fibrillation in a population-based cohort. The Framingham Heart Study. J Am Med Assoc 1994;271:840–4.
[8] Wang TJ, Parise H, Levy D, et al. Obesity and the risk of new-onset atrial fibrillation. J Am Med Assoc 2004;292:2471–7.
[9] Watanabe H, Tanabe N, Watanabe T, et al. Metabolic syndrome and risk of development of atrial fibrillation: the Niigata preventive medicine study. Circulation 2008;117:1255–60.
[10] Sanders P, Morton JB, Kistler PM, et al. Electrophysiological and electroanatomic characterization of the atria in sinus node disease: evidence of diffuse atrial remodeling. Circulation 2004;109:1514–22.
[11] Lin YJ, Tai CT, Kao T, et al. Spatiotemporal organization of the left atrial substrate after circumferential pulmonary vein isolation of atrial fibrillation. Circ Arrhythm Electrophysiol 2009;2:233–41.
[12] Okumura Y, Watanabe I, Kofune M, et al. Characteristics and distribution of complex fractionated atrial electrograms and the dominant frequency during atrial fibrillation: relationship to the response and outcome of circumferential pulmonary vein isolation. J Interv Card Electrophysiol 2012;34:267–75.
[13] Gerstenfeld EP, Lavi N, Bazan V, et al. Mechanism of complex fractionated electrograms recorded during atrial fibrillation in a canine model. Pacing Clin Electrophysiol 2011;34:844–57.
[14] Wijffels MC, Kirchhof CJ, Dorland R, et al. Atrial fibrillation begets atrial fibrillation. A study in awake chronically instrumented goats. Circulation 1995;92:1954–68.
[15] Hara M, Shvilkin A, Rosen MR, et al. Steady-state and nonsteady-state action potentials in fibrillating canine atrium: abnormal rate adaptation and its possible mechanisms. Cardiovasc Res 1999;42:455–69.
[16] Allessie M, Ausma J, Schotten U. Electrical, contractile and structural remodeling during atrial fibrillation. Cardiovasc Res 2002;54:230–46.
[17] Jaïs P, Hocini M, Macle L, Choi KJ, et al. Distinctive electrophysiological properties of pulmonary veins in patients with atrial fibrillation. Circulation 2002;106:2479–85.
[18] Chen SA, Hsieh MH, Tai CT, et al. Initiation of atrial fibrillation by ectopic beats originating from the pulmonary veins: electrophysiological characteristics, pharmacological responses, and effects of radiofrequency ablation. Circulation 1999;100:1879–86.
[19] Munger TM, Dong YX, Masaki M, et al. Electrophysiological and hemodynamic characteristics associated with obesity in patients with atrial fibrillation. J Am Coll Cardiol 2012;60:851–60.

[20] Mora S, Akinkuolie AO, Sandhu RK, et al. Paradoxical association of lipoprotein measures with incident atrial fibrillation. Circ Arrhythm Electrophysiol 2014;7:612–9.
[21] Watanabe H, Tanabe N, Yagihara N, et al. Association between lipid profile and risk of atrial fibrillation. Circ J 2011;75:2767–74.
[22] Lopez FL, Agarwal SK, Maclehose RF, et al. Blood lipid levels, lipid-lowering medications, and the incidence of atrial fibrillation: the Atherosclerosis Risk in Communities Study. Circ Arrhythm Electrophysiol 2012;5:155–62.
[23] Ravelli F, Allessie M. Effects of atrial dilatation on refractory period and vulnerability to atrial fibrillation in the isolated Langendorff-perfused rabbit heart. Circulation 1997;96:1686–95.
[24] Bode F, Katchman A, Woosley RL, et al. Gadolinium decreases stretch-induced vulnerability to atrial fibrillation. Circulation 2000;101:2200–5.
[25] Kalifa J, Jalife J, Zaitsev AV, et al. Intra-atrial pressure increases rate and organization of waves emanating from the superior pulmonary veins during atrial fibrillation. Circulation 2003;108:668–71.
[26] Walters TE, Lee G, Spence S, et al. Acute atrial stretch results in conduction slowing and complex signals at the pulmonary vein to left atrial junction: insights into the mechanism of pulmonary vein arrhythmogenesis. Circ Arrhythm Electrophysiol 2014;7:1189–97.
[27] Zipes DP, Mihalick MJ, Robbins GT. Effects of selective vagal and stellate ganglion stimulation of atrial refractoriness. Cardiovasc Res 1974;8:647–55.
[28] Patterson E, Po SS, Scherlag BJ, et al. Triggered firing in pulmonary veins initiated by *in vitro* autonomic nerve stimulation. Heart Rhythm 2005;2:624–31.
[29] Asghar O, Alam U, Hayat SA, et al. Obesity, diabetes and atrial fibrillation; epidemiology, mechanisms and interventions. Curr Cardiol Rev 2012;8:253–64.
[30] Zhang Y, Wang YT, Shan ZL, et al. Role of inflammation in the initiation and maintenance of atrial fibrillation and the protective effect of atorvastatin in a goat model of aseptic pericarditis. Mol Med Rep 2015;11:2615–23.
[31] Abed HS, Samuel CS, Lau DH, et al. Obesity results in progressive atrial structural and electrical remodeling: implications for atrial fibrillation. Heart Rhythm 2013;10:90–100.
[32] Atienza F, Calvo D, Almendral J, et al. Mechanisms of fractionated electrograms formation in the posterior left atrium during paroxysmal atrial fibrillation in humans. J Am Coll Cardiol 2011;57:1081–92.
[33] Jadidi AS, Duncan E, Miyazaki S, et al. Functional nature of electrogram fractionation demonstrated by left atrial high-density mapping. Circ Arrhythm Electrophysiol 2012;5:32–42.
[34] Miyamoto K, Tsuchiya T, Nagamoto Y, et al. Characterization of bipolar electrograms during sinus rhythm for complex fractionated atrial electrograms recorded in patients with paroxysmal and persistent atrial fibrillation. Europace 2010;12:494–501.